Computational and Structural Biotechnology Journal 21 (2023) 5785–5795

Contents lists available at ScienceDirect

Computational and Structural Biotechnology Journal

journal homepage: www.elsevier.com/locate/csbj

Research Article

Adaptive control of the *E. coli*-specific growth rate in fed-batch cultivation based on oxygen uptake rate

Renaldas Urniezius *, Deividas Masaitis, Donatas Levisauskas, Arnas Survyla, Povilas Babilius, Dziuljeta Godoladze

Department of Automation, Kaunas University of Technology, Studentu 48, LT-51367 Kaunas, Lithuania

ARTICLE INFO

Keywords:
Fed-batch culture
Specific growth rate
Setpoint control
Adaptive control

ABSTRACT

In this study, an automatic control system is developed for the setpoint control of the cell biomass specific growth rate (SGR) in fed-batch cultivation processes. The feedback signal in the control system is obtained from the oxygen uptake rate (OUR) measurement-based SGR estimator. The OUR online measurements adapt the system controller to time-varying operating conditions. The developed approach of the PI controller adaptation is presented and discussed. The feasibility of the control system for tracking a desired biomass growth time profile is demonstrated with numerical simulations and fed-batch culture *E. coli* control experiments in a laboratory-scale bioreactor. The procedure was cross-validated with the open-loop digital twin SGR estimator, as well as with the adaptive control of the SGR, by tracking a desired setpoint time profile. The digital twin behavior statistically showed less of a bias when compared to SGR estimator performance. However, the adaptation—when using first principles—was outperformed 30 times by the model predictive controller in a robustness check scenario.

1. Introduction

The production of target products (pharmaceuticals, enzymes, recombinant proteins, stem cells, and mammalian cells) by fed-batch cultures at high yields and quality is closely related to the cellular biomass-specific growth rate (SGR) [1–3]. Accurate control of the SGR improves the reproducibility of cultivation processes, and it is also critical for optimizing existing biosyntheses, as well as for developing new biosyntheses, in producing desirable products.

It should be stressed that the SGR is not directly measured, and the adaptation of the system controller to the time-varying dynamics of fed-batch cultivation processes is necessary. Developing reliable SGR control systems is not a trivial task, and examples of SGR control schemas are rare in industrial applications.

The mainstream approach for SGR control depends on biomass concentration observations (see first row, Fig. 1, [4–7,9,10,19]), secreted metabolite concentrations (see fifth row, Fig. 1, [21–26]), or off-gas analysis-based information (sixth row, Fig. 1, [8,12,15–18]). Historically, a straightforward SGR control at a desired setpoint has been implemented with open-loop control systems. These systems are usually utilized in a conventional exponential feeding strategy [4,5,27], in which the pattern of the controlled process can be considered, for example, by the loss of biomass induced by the foaming [5]. However, these systems do not ensure accurate control when there are process-state variable deviations that change directions from the desired paths. Experimental investigations of open-loop control system performance for controlling the SGR in recombinant *E. coli* fed-batch cultures show significant deviations of 14-19% of the controlled SGR from the setpoints at low setpoint values [4].

The biomass concentration estimate-based SGR control systems are developed through biomass concentration online estimates, which are obtained by using advanced instrumentation such as dielectric spectroscopy (Raman) and heat rate measurements. Dielectric spectroscopy is sensitive to viable biomass, and the SGR is computed using biomass concentration measurements [9,10]. The measurement device must be calibrated for each cell strain and culture condition. In control systems [9,10], modified feed-forward/feedback control algorithms are dedicated to increasing the system's performance when under exponential biomass growth dynamics. Experimental investigations of the proposed heuristic algorithms show limited control precision and noticeable oscillations when tracking the SGR setpoint. These control systems can be applied for various fed-batch cultures with minor modifications. In

* Corresponding author.
E-mail address: renaldas.urniezius@ktu.lt (R. Urniezius).

https://doi.org/10.1016/j.csbj.2023.11.033
Received 10 August 2023; Received in revised form 17 November 2023; Accepted 17 November 2023
Available online 23 November 2023
2001-0370/© 2023 The Author(s). Published by Elsevier B.V. on behalf of Research Network of Computational and Structural Biotechnology. This is an open access article under the CC BY-NC-ND license (http://creativecommons.org/licenses/by-nc-nd/4.0/).

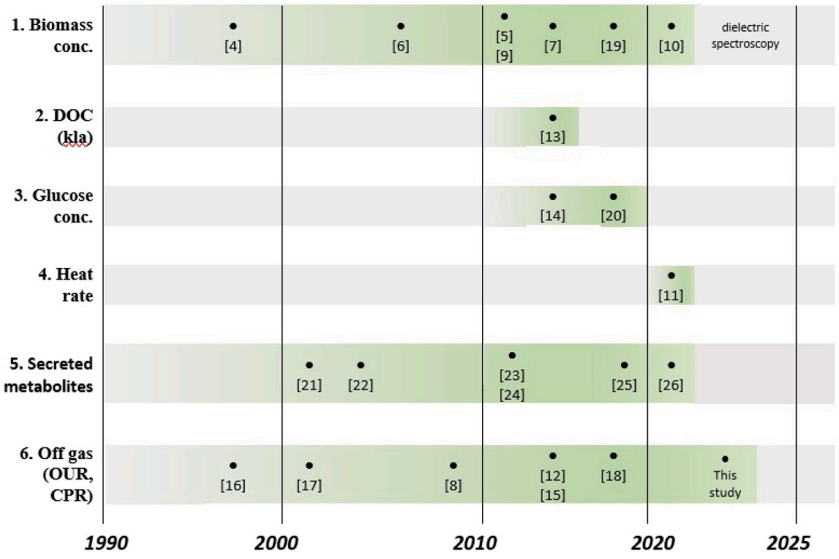

Fig. 1. The chronological view of the SGR control progress with a distinct feedback signal per development (row).

[14], a nonlinear bioprocess model was developed to represent the CHO mammalian cell fed-batch cultivation process. This model was applied for the setpoint control of glucose concentration [20] in bioreactors, and this was achieved using the Model Predictive Control (MPC) approach. The proposed controller allowed for relatively good results with respect to glucose concentration control in the bioreactor. However, because of the non-stationary and non-linear relationship between glucose concentration and the specific growth rate, the regulation of the fixed setpoint profile of glucose concentration gave different values for the SGR in different cultivation runs. An SGR control system that utilizes a metabolic heat rate signal was developed in [11]. The heat rate was used for the online estimation of an SGR feedback signal, which was applied in a feed-forward/feedback control system with a gain-scheduled PID controller. Such a system was only limited by its applicability in specialized bioreactors, in which the heat compensation calorimeter was available. Experimental investigations were required to determine the control system performance for the control of P. Furthermore, pastoris fed-batch cultures at a steady setpoint have shown satisfactory results. However, the performance of the heat rate-based SGR estimator was not capable of being illustrated through a comparison of the estimates, and the actual SGR time trajectories at a setpoint step changed when transient conditions occurred.

Application of the dissolved oxygen concentration (DOC) for the SGR setpoint control was proposed in [13]. In such a bioreactor control system, the DOC is controlled using a cascade control system. In addition, the SGR is restricted to a steady setpoint by a model reference adaptive controller, the adaptation of which considers the estimated biomass concentration and volume of cultural liquid. The working capacity of the SGR control system was confirmed by fed-batch culture $B.pertussis$ simulation and laboratory experiments. In order to avoid the oscillatory behavior of the SGR control due to interactions with the DOC control system, the controller-tuning parameters need to be correctly determined.

In the present work, a control system was developed to automatically control fed-batch cultures at desired biomass SGR time profiles, thereby requiring no optimum search implementations to control the process. In this control system, the OUR-based SGR estimators developed by the authors were tested for the online calculation of a feedback signal [28]. The OUR measurements were also used for the SGR controller adaptation to time-varying operating conditions. The motivation was that local concentration-oriented observations and their affordable sensors face non-homogeneous media [29,30], or morphological change [31] issues when biomass concentrations are too high or too low.

Section 1 discusses the motives for using an adaptive control system with feedback from the SGR; Section 2 analyzes the literature relevant to this work; Section 3 describes the details of the bioreactor system, SGR estimation procedure, and development of the adaptive control system; Section 4 outlines the digital twin model of a cultivation process; Section 5 lays out results of the control system and compares them with the experimental data; and the final section presents the conclusions of this study.

2. Related works

The trade-off in existing control systems is that estimating the SGR, as based on biomass concentration and handling the rapid SGR setpoint variations, might become challenging [32]. The proposed partial-state feedback controllers with adjustable gains were developed using tendency models of a controlled process, as well as by utilizing the knowledge of process parameters.

The SGR feedback signal was calculated using the Luedeking–Piret-type relationship [33,34] and the OUR online measurements in these systems. In the first control system, a model-based adaptation algorithm of the PI controller was developed using a mathematical model developed for the recombinant $E.coli$ cultivation process. This model uses the OUR as a gain-scheduling variable. In the adaptation algorithm, the steady-state operating condition of the substrate concentration, as well as the constant value of the derivative $\partial\mu/\partial s$, were assumed. Such assumptions will, however, decrease the accuracy of controller adaptation when greater SGR setpoint changes occur. In the second control system, tuning the ANN-based controller parameters requires a sufficient amount of statistical experimental data. The process model-based simulations of the control system performance show that such systems deliver comparable control performances, and that they are suitable for applications that are subjected to growth-limiting substrate conditions. However, the simulation results have not yet been qualified by relevant laboratory experiments.

This study is a continuation of SGR control developments, in which information for SGR control is obtained from an off-gas analyzer. The equipment for exhaust gas analysis provides information for the online estimation of the oxygen uptakes and carbon dioxide production rates (OUR and CPR, respectively) that are used in the SGR control systems for the feedback signals [8,16,17,26], controller adaptation [33], and in the control of the growth rate at desired time profiles [8,12,15,35]. In [8], the control of the SGR was completed by using the generic model control (GMC) approach, which requires an accurate model of the con-

trolled process and reliable online estimates of the following indirectly assessed state variables: the SGR, biomass, and the substrate concentrations that are computed using OUR, CPR, and amount of base required for pH control. The system provided good results in a pilot bioreactor. However, these good results were achieved at the expense of model and measurement system development. In [12], the cascade control system was developed, which can hold the SGR time profile at a desired profile during the fed-batch processes of recombinant protein production. The system directly controls the CPR and the cumulative amount of carbon dioxide at predetermined time trajectories, thus keeping the SGR and biomass growth trajectories at the desired paths. To apply the control system, the reference time trajectories of the controlled variables are to be determined in advance. In [15], the MPC strategy was applied to control the SGR in the animal cell (CHO-cell) suspensions that were cultivated for recombinant protein production. In [36], the integration of MPCs with a moving horizon estimation (MHE) framework was employed to enhance *E. coli* growth. This strategy efficiently fine-tuned the feeding system, thus yielding the intended outcomes. However, the intricate nature of cell metabolism introduces variability in the kinetic parameters that exist across diverse cultivation conditions, or can produce performance issues when optimum search implementations are necessary. An optimal SGR was maintained indirectly by manipulating the glutamine feed rate and controlling the oxygen consumption at desired time trajectories.

The off-gas based systems were developed for controlling the SGR at a steady setpoint. In the control systems, the estimated ratio $R = (\mathrm{d}OUR/\mathrm{d}t)/OUR$ (d is a differential operator), which asymptotically approached the SGR at steady setpoint control conditions, was used as a feedback signal in the SGR control loops. Such systems are well-suited for keeping the SGR at a steady setpoint. However, they fail to control the SGR at the desired time-varying trajectories as there is no coincidence between the ratio R and the SGR at transient conditions. Due to this reason, certain oscillations in the control system also occur due to controlling the SGR at a steady setpoint [17]. The digital twin of this study is a focus object that was obtained by additionally testing it with the MPC algorithm. The purpose was to compare two distinct candidate control algorithms, as well as to find the trade-offs in both. We assumed that our control strategy considered avoiding the overflow metabolism by design.

3. Materials and methods

3.1. Cell strains and cultivation conditions

The SGR control system and digital twin models were investigated based on the data from the cultivation process of *Escherichia coli* (*E. coli*) bacteria. A total of two bacterial strains were employed.

- *E. coli* BL21 (DE3) pET21-IFN-alfa-5;
- *E. coli* BL21 (DE3) pET28a.

E. coli BL21 (DE3) pET21-IFN-alfa-5 bacteria were grown in a minimal mineral medium, and the cultivation process protocol, as described in the research of [37], is shown in Table 1. The oxygen concentrations' online measurements, ranging from 0 to 100%, were retrieved using the BlueSens BlueInOne Ferm gas analyzer for oxygen uptake rate evaluation. The gas analyzer had an approximately 0.2% error. The airflow information data were taken from the Applikon BioBundle bioreactor.

E. coli BL21 (DE3) pET28a bacteria were also grown in a minimal mineral medium, and the bioreactor growth protocol, as described in prior research [38], is stated in Table 2. To detect the oxygen uptake rate, a thermal mass flow controller (Bronkhorst–Mattig) was employed with a paramagnetic oxygen sensor (Maihak Oxor 610), and this was then placed in the reactor vent behind the off-gas condenser.

Table 1
E. coli BL21 (DE3) pET21-IFN-alfa-5 cultivation details.

Condition	State	Condition	State
Bioreactor volume	7 L	Broth volume	3.7 kg
Temperature	37 °C	pH	6.8
pO2	20%	Feeding start	at 5-7 h
Stirrer	800-1200 RPM	Induction time	at 11-13 h

Table 2
E. coli BL21 (DE3) pET28a cultivation details.

Condition	State	Condition	State
Bioreactor volume	10 L	Broth volume	5 kg
Temperature	35 °C	pH	7
pO2	25%	Feeding start	at 4-6 h
Stirrer	100-1400 RPM	Induction time	at 9-10 h

In this study, the difference in the oxygen concentrations between the intake air flow and the bioreactor exhaust gas was used to calculate the oxygen uptake rate (OUR) [39]:

$$OUR(t) = \frac{Q(t) \cdot (O_2^{in}(t) - O_2^{out}(t)) \cdot M_{O_2}}{V_m \cdot W(t) \cdot 100}, \tag{1}$$

where O_2^{in} and O_2^{out} are the oxygen concentrations of inlet and outlet gas flows, %; Q is the gas flow rate, L/h; W is working volume of the bioreactor, kg; V_m is the molar volume, mol/L; and M_{O_2} is molar mass of oxygen, g/mol.

3.2. Specific growth rate estimator

An SGR feedback signal based on the Luedeking–Piret model is essential for developing an SGR automatic control system [40].

$$OUR(t) = \alpha \cdot x'(t) + \beta \cdot x(t), \tag{2}$$

where x is the biomass concentration (g kg^{-1}), t is the time (h), OUR is the oxygen uptake rate (g kg^{-1} h^{-1}), and $\alpha \equiv Y_{o/x}$ (g g^{-1}) and β (g g^{-1} h^{-1}) are the stoichiometry parameters that determine the growth and maintenance properties of biomass. The SGR estimation procedure suggested in this study originates from biomass concentration estimates that were based on a bioreactor exhaust gas analysis [41,28]. The chosen method exhibited stability in estimating biomass concentrations at various cultivation conditions. The estimator evaluates the online biomass concentration from the oxygen uptake rate (OUR) estimates, as well as providing a feedback signal for a SGR controller. In the research of [28], an estimator for biomass concentration was developed and investigated. The selected model described the evaluation of the process as follows:

$$\hat{x}_i = \frac{x_0 + \sum_{j=1}^{i} \frac{OUR(t_j)}{Y_{o/x}} e^{\sum_{k=1}^{j} \frac{\beta(t_k)}{Y_{o/x}} \triangle t_k} \triangle t_j}{e^{\sum_{j=1}^{i} \frac{\beta(t_j)}{Y_{o/x}} \triangle t_j}}, \tag{3}$$

where $\hat{x}$ is the estimated biomass concentration (g kg^{-1}), and the boundary value x_0 is the biomass concentration at inoculation time. In the study of [28], the parameter β depended on biomass concentration rather than the assumed constant.

$$\beta(t_i) = \begin{cases} 0, & \text{if } \sum_{k=1}^{i} x(t_k)\, \mathrm{d}t_k \le k_{cX} \\ \frac{m \cdot (x(t_i) - x_{cX})}{x(t_i)}, & \text{otherwise} \end{cases} \tag{4}$$

where m is the biomass maintenance term, and k_{cX} is a parameter that describes the time moment t_{cX} when the stoichiometry parameter β is no longer equal to zero, as well as when the biomass concentration

x_{cX} corresponds to the time when the following conditions hold $k_{cX} \equiv \sum_{j=1}^{t_j=t_{cX}} x(t_j) \triangle t_j, x_{cX} \equiv x(t_{cX})$.

An issue with the stoichiometry parameter β was discovered during the investigation of the *E. coli* BL21 (DE3) pET28a strain, which is characterized by a high-protein-synthesis capacity. The β parameter was constructed using *E. coli* BL21 (DE3) pET21-IFN-alpha-5 culture strain data, which has a significantly lesser efficacy in protein synthesis than the *E. coli* BL21 (DE3) pET28a strain. Following induction (using, for example, isopropyl-d-1-thiogalactopyranoside/IPTG), cells start synthesizing products with the use of more oxygen. Including an additional stoichiometry parameter γ, which reflects the oxygen consumption for protein synthesis, is the means through which to adapt the stoichiometry parameter β (Equation (4)) model to the highest efficiency of protein production. The model of protein synthesis yielding γ was taken from the research of [38].

$$\gamma(x) = k_\gamma \cdot (x(t) - x_{ind}), \tag{5}$$

where k_γ is the yield of the product synthesis, which is considered constant. x_{ind} is the biomass concentration at induction time moment t_{ind}. In order to apply Equation (5) to the stoichiometry parameter β (Equation (4)), the γ parameter (Equation (5))—which was obtained from the research of [38]—was normalized as shown below:

$$\gamma^*(x) \equiv \frac{\gamma(x)}{x(t)} = \frac{k_\gamma \cdot (x(t) - x_{ind})}{x(t)}, \tag{6}$$

where $\gamma^*(x)$ is normalized over the biomass concentration. Hence, the product synthesis led to the addition of the protein production component $\gamma^*(x)$ to the model of the stoichiometric parameter β. Currently, the β parameter value is based on the bioprocess current state:

$$\beta\left(t_i\right) = \begin{cases} 0, \text{if } \sum_{k=1}^{i} x\left(t_k\right) \mathrm{d}t_k \le k_{cX}, \\ \frac{m(x(t_i) - x_{cX})}{x(t_i)} + \begin{cases} 0, \text{if } \sum_{k=1}^{i} x\left(t_k\right) \mathrm{d}t_k > k_{cX} \text{ and } t \le t_{ind}, \\ \gamma^*(x), \text{otherwise}, \end{cases} \end{cases} \tag{7}$$

where t_{ind} is the induction time. The suggested definition of the stoichiometry parameter β in Equation (7) aims to preserve the original structure of the biomass concentration estimation model (Equation (3)). The specific growth rate values for the SGR control system were obtained in conjunction with the evaluation of the biomass concentration. The following equation was used to calculate the SGR for the time interval $\triangle t_i \equiv t_{i,i-1} = t_i - t_{i-1}$ [42]:

$$\mu(t_i) \equiv \mu(t_{i,i-1}) = \frac{ln(\frac{x(t_i)}{x(t_{i-1})})}{\triangle t_i}, \tag{8}$$

where μ is the specific growth rate.

3.3. Gain scheduling for the SGR controller adaptation

3.3.1. Adaptive transfer function of the controlled process

Ordinary feedback control systems with fixed-gain PID (PI) controllers cannot handle accurate control challenges for the SGR due to significant variations in the controlled process of the dynamics that occur throughout the fed-batch biosynthesis. As a result, a controller adaptation to time-varying operating conditions is required to increase the control system's performance. The adaptation is based on exploiting a tendency model that describes the essential dynamical features of the controlled process as follows:

$$\frac{\mathrm{d}s}{\mathrm{d}t} = \frac{\mu(s)}{Y_{s/x}} x + u \frac{s_f - s}{W}, \tag{9}$$

$$\mu(s) = \frac{\mu_{max} \cdot s}{s + k_s}, \tag{10}$$

where s is the substrate concentration; u is the feeding rate (manipulated variable); s_f is the feeding substrate concentration; and μ_{max}, k_s, $Y_{s/x}$ are the specific constants that are dependent on cell culture. Equation (9) represents the mass balance for the substrate, and Equation (10) represents the Monod relationship that relates to a specific growth rate for substrate concentration [43].

The linearization of the model's Equations (9) and (10) at the state points of the variables s and u—which were sampled on t_k—lead to the following equations:

$$\frac{\mathrm{d}(\triangle s)}{\mathrm{d}t} = -\left(\frac{x}{Y_{s/x}} \frac{\partial \mu(s)}{\partial s} + \frac{u}{W}\right)_{t=t_k} \triangle s + \left(\frac{s_f - s}{W}\right)_{t=t_k} \triangle u, \tag{11}$$

$$\triangle \mu = \left(\frac{\mu_{max} \cdot k_s}{(s + k_s)^2}\right)_{t=t_k} \triangle s, \tag{12}$$

where $\triangle s$ and $\triangle u$ denote the small deviations of s and u from the state point values at time t_k.

The linear Equations (11) and (12) describe the controlled process dynamics along the process's trajectory. From the above equations, the following transfer function models of the process can be derived:

$$G_{\triangle s/\triangle u}(p) = \frac{\triangle s(p)}{\triangle u(p)} = \frac{K_{\triangle s/\triangle u}(t_k)}{T_{\triangle s/\triangle u}(t_k)p + 1}, \tag{13}$$

$$G_{\triangle \mu/\triangle s}(p) = \frac{\triangle \mu(p)}{\triangle s(p)} = K_{\triangle \mu/\triangle s}(t_k), \tag{14}$$

where

$$K_{\triangle s/\triangle u}(t_k) = \frac{s_f - s(t_k)}{\frac{x(t_k)W(t_k)}{Y_{s/x}} \frac{\partial \mu}{\partial s}(t_k) + u(t_k)}, \tag{15}$$

$$T_{\triangle s/\triangle u}(t_k) = \frac{W(t_k)}{\frac{x(t_k)W(t_k)}{Y_{s/x}} \frac{\partial \mu}{\partial s}(t_k) + u(t_k)}, \tag{16}$$

$$K_{\triangle \mu/\triangle s}(t_k) = \frac{\partial \mu}{\partial s}(t_k) = \frac{\mu_{max} k_s}{\left(s(t_k) + k_s\right)^2}, \tag{17}$$

where p is the Laplace operator; $K_{\triangle s/\triangle u}$ and $K_{\triangle \mu/\triangle s}$ are the gain coefficients; and $T_{\triangle s/\triangle u}$ is the time constant of the controlled process.

The transfer function models (13) - (17) representing the first-order dynamics of the controlled process should also be supplemented with a time-delay term τ_{pr}. This term helps with estimating the delay of the SGR's reaction with respect to the substrate concentration change dynamics and other possible delays in the control system elements—aspects that are not taken into account in the simplified first principles model (9), (10).

The resultant transfer function of the controlled process takes the form of the first-order plus time delay model:

$$G_{\triangle \mu/\triangle u}(p) = \frac{\triangle \mu(p)}{\triangle u(p)} = G_{\triangle \mu/\triangle s}(p) \cdot G_{\triangle s/\triangle u}(p) \cdot exp(-\tau_{pr} p) = \frac{K_{pr}(t_k)}{T_{pr}(t_k)p + 1} exp(-\tau_{pr} p), \tag{18}$$

where $K_{pr}(t_k)$ is the resultant gain coefficient ($K_{pr}(t_k) = K_{\triangle \mu/\triangle s}(t_k) \cdot K_{\triangle s/\triangle u}(t_k)$); $T_{pr}(t_k)$ is the resultant time constant ($T_{pr}(t_k) = T_{\triangle s/\triangle u}(t_k)$); and τ_{pr} is the resultant time delay. The total amount of biomass (xV) at time t_k in the relationships (15) and (16) can be indirectly estimated online from the OUR measurements via the following relationship:

$$\frac{\mathrm{d}(xW)}{\mathrm{d}t} \cong Y_{o/x} OUR, \tag{19}$$

$$x(t_k)W(t_k) \cong Y_{o/x} \int_{t_0}^{t_k} OUR \mathrm{d}t, \tag{20}$$

where $Y_{o/x}$ is the biomass yield coefficient concerning the oxygen found in reference sources, or is estimated from previous experiments.

For computing the expression (17), the transfer function parameter $K_{\triangle\mu/\triangle s}$ and the derivative $\partial\mu/\partial s(t_k)$ values in the relationships (15), (16), and the online measurements of the substrate concentration $s(t_k)$ are necessary. As the substrate concentration is not directly measured, it can be indirectly estimated from the Monod relationship (10) by equating it to the estimated value of the controlled SGR ($\hat{\mu}$, which is where the hat operator is used to denote the estimator or estimated value):

$$s(t_k) = \frac{k_s\hat{\mu}(t_k)}{\mu_{max} - \hat{\mu}(t_k)}. \tag{21}$$

By substituting (20) and (21) into Equations (15)-(17), as well as by taking into account the significant distinctions in the term values in Equations (15) and (16), $s_f \gg s(t_k)$, and $\frac{x(t_k)W(t_k)}{Y_{s/x}}\frac{\partial\mu}{\partial s}(t_k) \gg u(t_k)$, the transfer function (18) parameters can be roughly assessed from the following relationships:

$$K_{pr}(t_k) \cong \frac{s_f Y_{s/x}}{Y_{o/x}\int_{t_0}^{t_k} OUR\,\mathrm{d}t}, \tag{22}$$

$$T_{pr}(t_k) \cong \frac{Y_{s/x}\mu_{max}k_s W(t_k)}{Y_{o/x}(\mu_{max} - \hat{\mu}(t_k))^2\int_{t_0}^{t_k} OUR\,\mathrm{d}t}, \tag{23}$$

where parameters μ_{max}, k_s, $Y_{s/x}$, and $Y_{o/x}$ can be found in reference sources, or they can be estimated from previous experiments.

If the dynamic process parameters (22) and (23) are updated online with the measured values of the volume, OUR and the SGR, the transfer function model (18) follows the time-varying state of the controlled process; moreover, they can also be directly applied for the online adaptation of the SGR controller parameters.

3.3.2. Controller adaptation

The PI controller was used in the developed SGR control system, and this was less sensitive to feedback signal noise than the PID controller.

The transfer function model (18)—which was updated online with the estimated values of parameters $K_{pr}(t_k)$ and $T_{pr}(t_k)$—was directly applied for the adaptation of the PI controller to the time-varying state of the controlled process, and this was achieved using the controller tuning rules that were developed for dynamic models. In this way, the controller parameters were recalculated at each control sampling step, and the mismatch between the process state and controller settings (which occurs in a conventional control system) was avoided.

We applied the Kappa-Tau tuning rules to develop the SGR controller adaptation [44]. In the SGR control system, the PI controller tuning rules for a maximum sensitivity of $M_s = 1.4$ were used:

$$K_c(t_k) = 0.29\frac{T_{pr}(t_k)}{K_{pr}(t_k)\tau_{pr}}exp(-2.7\tau(t_k) + 3.7\tau(t_k)^2), \tag{24}$$

$$T_i(t_k) = 0.79T_{pr}(t_k)exp(-1.4\tau(t_k) + 2.4\tau(t_k)^2), \tag{25}$$

$$b(t_k) = 0.79exp(-1.4\tau(t_k) + 2.4\tau(t_k)^2), \tag{26}$$

$$\tau(t_k) = \frac{\tau_{pr}}{\tau_{pr} + T_{pr}(t_k)}, \tag{27}$$

where K_c is the controller gain, T_i is the integral time constant, and b is the setpoint weight factor (i.e., the tuning parameter of the modified PI control [44]) that was estimated at time t_k.

By substituting the transfer function (18), the parameter values were retrieved from Equations (22) and (23) into the tuning rules (24)-(27); as such, the formulas for the controller adaptation were derived. The trial-and-error technique can improve the controller tuning parameters in the above formulas.

The block scheme of the SGR adaptive control system is depicted in Fig. 2.

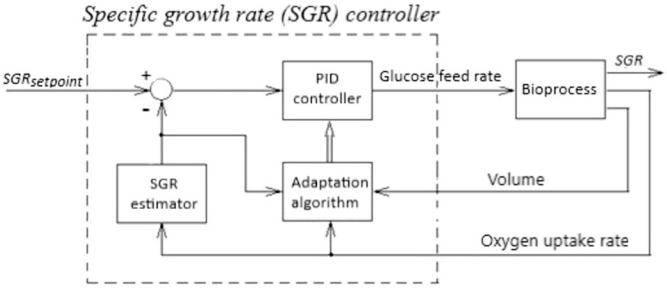

Fig. 2. Block scheme of the SGR adaptive control system.

4. Investigation of the SGR control system performance

4.1. Digital twin

The performance of the SGR control system shown in Fig. 2 was initially investigated using numeric simulations. The simulation experiments were simulated in a MATLAB/Simulink environment. In the tests, a parametric model (digital twin) of the *E. coli* fed-batch cultivation process was used to simulate the controlled biosynthesis as follows:

$$\frac{\mathrm{d}x}{\mathrm{d}t} = \mu(s)\cdot x(t) - F(t)\frac{x(t)}{W(t)}, \tag{28}$$

$$\frac{\mathrm{d}s}{\mathrm{d}t} = -q_s(s)x(t) - F(t)\frac{s(t)}{W(t)} + u(t)\frac{s_f}{W(t)}, \tag{29}$$

$$\frac{\mathrm{d}W}{\mathrm{d}t} = F(t) - F_{smp}, \tag{30}$$

$$F(t) = u(t) + F_b(t) + F_e(t), \tag{31}$$

$$F_b(t) = Y_{xb}\cdot\mu(s)\cdot x(t)\cdot W(t), \tag{32}$$

$$F_e(t) = -k_e\cdot W(t), \tag{33}$$

$$\mu(s) = \frac{\mu_{max}\cdot s(t)}{k_s + s(t)}, \tag{34}$$

$$q_s(s) = \begin{cases} \left(\frac{\mu(s)}{Y_{x/s}}\right), & t \le t_{ind} \\ \left(\frac{\mu(s)}{Y_{x/s}} + Y_{s/p}\right), & \text{otherwise} \end{cases} \tag{35}$$

$$OUR(t) = \mu(s)\cdot x(t)\cdot Y_{o/x} + \begin{cases} 0, \text{if } \int_0^t x(t^*)\mathrm{d}t^* \le k_{cX} \\ m(x(t) - x_{cX}) + \begin{cases} \gamma(x), & t \ge t_{ind} \\ 0, & \text{otherwise} \end{cases} \end{cases} \tag{36}$$

where q_s is the specific substrate consumption rate g g^{-1} h^{-1}, and $Y_{s/p}$ is the constant tuning coefficient. F_{smp} is the amount lost during sampling, kg/hr; F_b is an alkaline solution for pH control, kg/hr; F_e is the evaporation of the medium through the vent line, kg/hr; Y_{xb} is the parameter that represents the necessity of the alkali solution to the control pH due to the cell growth; and k_e is the coefficient of the nutritional medium evaporation.

Equations (28)-(30) are differential formulas of the main cultivation process variables [17,45]. Equation (34) is the same Monod expression as in Equation (10), in terms of having its digital twin and observer both depending on the identical object model. When the cultivation method includes induction (IPTG), Equation (35) is a more suitable version of the glucose consumption formula than the classical one [17]. Before induction, biomass maintenance is negligibly low or equal to zero; after product synthesis begins following induction, glucose consumption rises rapidly [38]. Equation (36) is taken from the study of biomass estimation [28,38], which is when the oxygen consumption maintenance term is significant after a specific biomass accumulation k_{cX} and when the glucose consumption term appears after induction.

The simulation system includes an additional element through which to prevent the model from reaching the unachievable condition where the glucose concentration cannot become negative. The element is a condition where the glucose consumption cannot exceed the glucose concentration in the bioreactor $q_s(s)x(t)\mathrm{d}t \le s(t)$. In such a case, when the glucose consumption is greater than the glucose concentration, then the specific cell growth rate is recalculated regarding the remaining glucose concentration in the bioreactor medium:

$$\mu(s) = \begin{cases} \left(\dfrac{s(t)\cdot Y_{x/s}}{x(t)\mathrm{d}t}\right), & t \le t_{ind} \\ \left(\dfrac{s(t)\cdot Y_{x/s}}{x(t)\mathrm{d}t}\right) - Y_{s/p}Y_{x/s}, & \text{otherwise} \end{cases} \tag{37}$$

Equation (37) is derived from Equation (35) by adding biomass and glucose concentrations.

The lag phase term was introduced to the simulation to make it more representative by enabling it to function from the start of the culture process. The cell culture cellular adaption, or lag phase, is when the biomass reproduction slowly reaches its total capacity. In the simulation, the specific growth rate parameter value is set to zero at the inoculation moment, and, after that, the cell reproduction slowly increases. An exponential filter defines the slow dynamics of the specific growth rate during the lag phase. The proposed expression has input values that originate from Equation (34) [46]:

$$\mu(t_k) = \mu(s)\cdot w + (1-w)\cdot \mu(t_{k-1}),\ t_k \le t_{lag} \tag{38}$$

where w is the numeric filter weight and t_{lag} is, approximately, the duration time of the lag phase. The weight of the exponential filter turns into one when the cultivation time surpasses the lag phase period.

Furthermore, the replication included Gaussian noise (with the percentage standard deviation σ set to 3%), and this was added to the OUR signal to make the simulated behavior more descriptive for controller verification than is the case for developed digital twin purposes.

4.2. Investigation of the SGR control using first principles

To investigate the performance of the SGR control, the digital twin assisted as the object, and the SGR estimator provided the necessary feedback signal. The time sampling step of the recursive SGR estimation and the discrete PI control was set to $\triangle t = 0.0166$ h in the simulation experiments. The control action of the SGR controller at each control sampling time point was calculated using the velocity from [47] regarding the following discrete PI control algorithm:

$$u(t_k) = u(t_{k-1}) + \triangle u(t_k), \tag{39}$$

$$\triangle u(t_k) = K_c(t_k)\left(e_b(t_k) + \frac{\triangle t_k}{T_i(t_k)}e(t_k) - e_b(t_{k-1})\right), \tag{40}$$

$$e_b(t_k) = b(t_k)\mu_{set} - \hat{\mu}(t_k), \tag{41}$$

$$e(t_k) = \mu_{set}(t_k) - \hat{\mu}(t_k), \tag{42}$$

where $u(t_k)$ is the control action (feeding rate) at time t_k; $\triangle t_k$ is the time sampling step of control actions ($\triangle t_k \equiv t_k - t_{k-1}$); $\mu_{set}(t_k)$ is the setpoint value of the specific growth rate at time t_k; $\hat{\mu}(t_k)$ is the estimated value of the specific growth rate; and $K_c(t_k)$, $T_i(t_k)$ and $b(t_k)$ are the PI controller parameters, which were determined at time t_k from the Kappa-Tau tuning rules (39)-(42). The controller compatibility with SGR estimation algorithms was demonstrated using the methodology from Section 3.2 as the feedback signal to the controller.

The values of the parameters that define cell culture essential information (28)-(38) are given in Table 3.

The values proposed in Table 3, as well as the initial values ($x_0 = 0.5$ g kg^{-1}, $s_0 = 5$ g kg^{-1}, $W_0 = 8$ kg), were taken from the research works of [17,28,42]. The controller parameter τ_{pr} was manually recalibrated in the cultivation process data of the *E. coli* BL21 (DE3) pET21-IFN-alfa-5 strain. The calibration result graphs of the controller are presented in Fig. 3. The digital twin and controller test performances are shown in Fig. 4.

Table 3
Model parameter values.

Parameters	Value	Dimension	Parameters	Value	Dimension
s_f	637	g kg^{-1}	k_s	0.07	g kg^{-1}
m	0.07	g g^{-1} h^{-1}	$Y_{x/s}$	0.4	g g^{-1}
$Y_{o/x}$	0.75	g g^{-1}	k_{cX}	17	g h kg^{-1}
μ_{max}	0.7	h^{-1}	w	0.02	-
t_{lag}	4	h^{-1}	k_γ	0.08	g g^{-1} h^{-1}
$Y_{s/p}$	0.035	g g^{-1}	t_{ind}	11-13	h
Y_{xb}	$7\cdot10^{-4}$	-	k_e	$5\cdot10^{-4}$	h^{-1}
λ	0.05	-	τ_{pr}	$5.5\cdot10^{-4}$	-

The simulated control system performances are presented in Figs. 3 and 4 (Experiments I and II). The SGR setpoint step-wise change time trajectory was used to investigate the controller adaptation at abrupt operating conditions. The results presented in Fig. 4 show that the control algorithm remains stable after Heaviside-like steps in the setpoint profile. Overshoot occurs when there is a sudden drop in the setpoint. At these types of moments, the algorithm has to cope with a considerable deceleration of the SGR.

4.3. Investigation of SGR control when using the MPC

The MPC analysis involved three efforts: digital twin modeling, optimization criteria selection [48,49], and the optimum search implementation. A digital twin is a prediction tool through which to obtain a reference glucose feeding profile (F_{ref}):

$$F_{ref_i} = \frac{q_s(s_i)}{S_f - s_i}\cdot x_{i-1}W_{i-1}e^{\mu_{sp_i}\triangle t_i}, \tag{43}$$

where x_0 and W_0 are the initial values in each iteration when assessing the F_{ref} profile, and μ_{sp} is the SGR value from the reference SGR profile. The next part of the MPC was responsible for evaluating the optimization criterion, as well as maintaining the reference trajectory during the process by minimizing the quadratic cost function, which is based on the errors between the reference and the online process value with a fixed number of samples $N_p = 10$ (where a sampled interval was one minute):

$$\Phi = \sum_{l=1}^{N_p}(\mu - \mu_{sp})^2 + \lambda\sum_{l=1}^{N_p}(u - F_{ref})^2 \tag{44}$$

where λ is the control penalty gain. Feed forward optimization was necessary for the MPC algorithm to adapt to the process. The convex optimization from [34] was chosen as the rational tool for the minimization of the Φ criteria:

$$min\ \Phi(\mu_n, u_n) \tag{45}$$

In Fig. 5, the MPC test results show satisfactory precision. However, in order to run the MPC, a monitoring program should run the digital twin with optimum search implementations ready, as makes this approach more complicated compared to the adaptive PI when using first principles.

5. Experimental investigation

The effectiveness and dependability of the SGR estimator and simulation (digital twin) were investigated with the data from the actual *E. coli* culture process. Out of all the trials, the growth-limiting feed rate experiments were chosen for analysis. The SGR regulation and digital twin were explored by a data analysis of the experiments with substrate feeding rates that resulted in various growth-limiting depths.

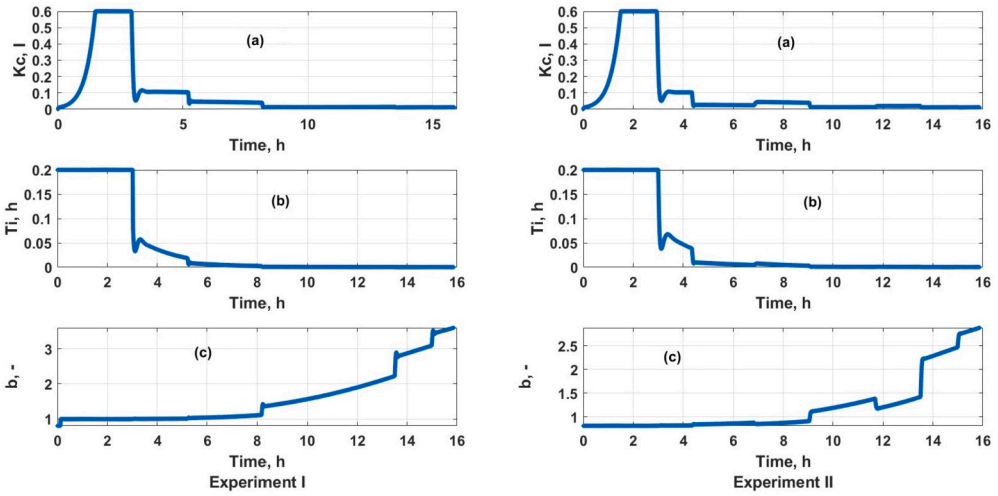

Fig. 3. Controller parameters: gain (a), integration time constant (b), and the setpoint weighting parameter (c).

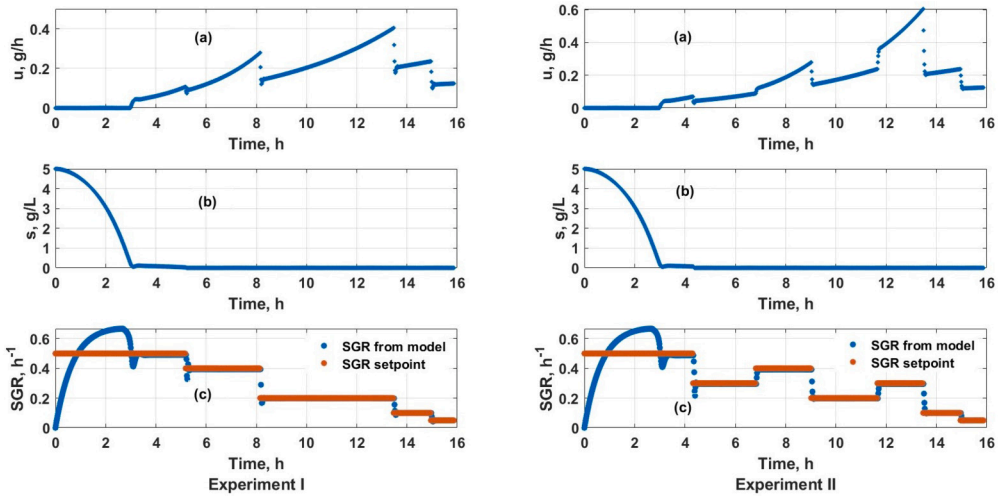

Fig. 4. Feeding rate (manipulated variable) (a); the glucose concentration in a bioreactor (b); the SGR controlled value (c).

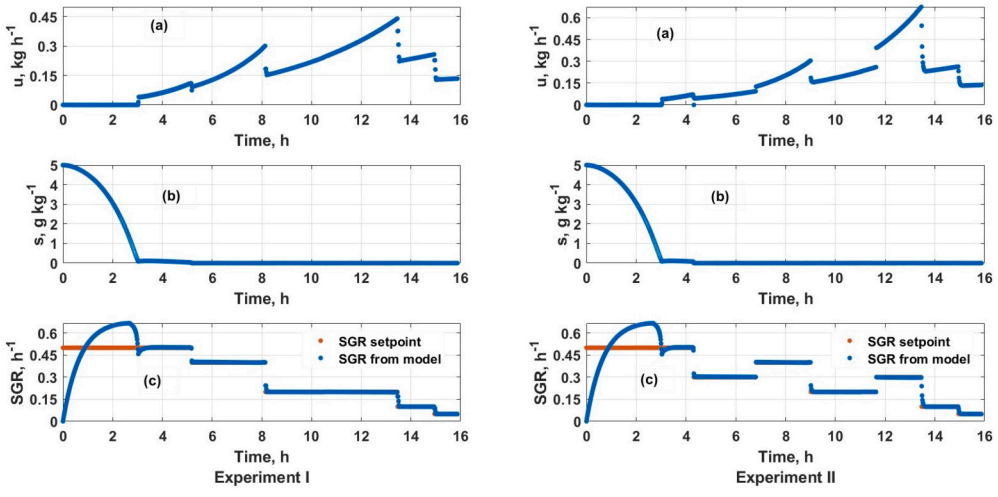

Fig. 5. MPC tests. The feeding rate (manipulated variable) (a); the glucose concentration in a bioreactor (b); and the SGR controlled value (c).

Table 4
E. coli BL21 (DE3) pET28a strain parameters for the digital twin model.

Parameters	Value	Dimension	Parameters	Value	Dimension
s_f	600	g kg^{-1}	k_s	0.1	g kg^{-1}
m	0.05	g g^{-1} h^{-1}	$Y_{x/s}$	0.75	g g^{-1}
$Y_{o/x}$	0.75	g g^{-1}	k_{cX}	17	g h kg^{-1}
μ_{max}	0.75	h^{-1}	w	0.013	-
t_{lag}	4	h^{-1}	k_γ	0.38	g g^{-1} h^{-1}
$Y_{s/p}$	0.03	g g^{-1}	t_{ind}	9-10	h

The comparison procedure was carried out in the following order:

1. A setpoint-specific growth rate profile was generated from the experimental data for each cultivation process test.
2. The initial cultivation conditions (x(0), s(0), and W(0)) of the inoculation moment were preset with observed values.
3. The SGR control (of this study) started action after receiving the first feedback from the digital twin infrastructure. The parameter values regarding the *E. coli* BL21 (DE3) pET21-IFN-alfa-5 strain's parameters are given in Table 3, and the *E. coli* BL21 (DE3) pET28a strain's parameters are presented in Table 4.
4. The SGR described in Section 3.2 was employed as the SGR feedback signal to the control system.
5. During the verification of the digital twin and controller repeatability, the system output was matched with the ground-truth data. In this check, the feedback signal originated from Equations (34) and (37). Other system signals also passed the consistency checks.

Setpoint profiles of the specific growth rates were generated using the experimental data and the SGR estimation technique (which are described in Section 3.2). During the validation tests, the indicator of the mean absolute error (MAE) and the normalized root mean square error (RMSE) was applied to describe the precision of the digital twin and the control of the SGR [50]:

$$MAE = \frac{\sum_{i=1}^{n} |\hat{y}_i - y_i|}{n}, \tag{46}$$

$$NRMSE = \frac{\sqrt{\frac{\sum_{i=1}^{n} (\hat{y}_i - y_i)^2}{n}}}{max(y) - min(y)}, \tag{47}$$

where n is the number of samples, $\hat{y}_i$ is the estimation and manipulated variable result, and y_i is a value that is measured or manipulated during cultivation. The suggested control system precision and the "Digital twin"-numeric behavior simulation results were demonstrated using the MAE and NRMSE precision criteria. In total, 15 cultivation process experiments were investigated in two different *E. coli* bacteria strains. The digital twin model results are shown in Table 5, and the whole systems that used the SGR estimator and the OUR model prediction are shown in Table 6.

Testing experiments that used actual data and two different types of feedback were accomplished so as to demonstrate the digital twin and controller numeric performances. A feedback outcome from the numerical models (Equations (34) and (37)) shows the precision of the controller and digital twin. The SGR estimation dictated an excess bias to the system response precision.

When comparing the results of the control systems from Table 5 and Table 6, the results showed that the SGR control performance was more precise when the feedback signal was evaluated in a less complicated manner (i.e., directly from the digital twin model, as in Table 5).

The average MAE of both the SGR control systems compared to the biomass concentration was 1.154 g kg^{-1}, and the NRMSE was 3.145%. The overall average MAE compared with the glucose concentration of both the SGR control systems was 0.175 g kg^{-1}, and the NRMSE was 4.831%. The average MAE of the OUR was 0.425 g kg^{-1} h^{-1}, the NRMSE was 5.238%, the overall average MAE of the substrate feeding rate was 4.756 g h^{-1}, and the NRMSE was 3.982%.

Fig. 6 displays experiment test number 3 of the *E. coli* BL21 (DE3) pET21-IFN-alfa-5 cell strain experiment. Fig. 7 graphically presents the results of experiment test number 5 of the *E. coli* BL21 (DE3) pET28a cell strain.

In Figs. 6 and 7, the confidence band values of $\alpha = 0.01$, the error bars of a systematic error of 0.2 g kg^{-1}, and a random error of 4% are shown. These errors reflect the bounds of the experimentation-related errors and device characteristics. The confidence band of the biomass was evaluated by comparing the experiment measurements and the estimated values. The errors were classified by biomass concentration to obtain the following:

$$\hat{e}(x) = 5.8 \cdot 10^{-4} x^2 + 9.767 \cdot 10^{-3} x. \tag{48}$$

Furthermore, the findings of this study, which were obtained using first principles, were also compared with previous MPC outcomes [49]. A comparison of the results is shown in Table 7, and this comparison proved that an adaption using first principles has a similar bias. However, there was one noticeable benefit in contrast to the MPC, which is that the adaptation of the PI does not require optimum search implementations in the manner that MPC does.

To compare the robustness of both the MPC and PI adaptations when using first principles, the culture-related controller parameters (Table 3 and 4) were randomized, the adaptation parameters were recomputed, and both systems were executed. The picked stress test scenario updated the inputs of the controller parameter values by artificially appending the RAND function $k = k + k \cdot Rand(-0.5, 0.5)$. The purpose was to simulate the situation where a less-known cell strain is being cultivated. The results of such an experiment were compared with the ground-truth process data, which are shown in Figs. 6 and 7. Both controllers managed to deal with the scenario, and the biomass concentration produced values that matched the ground truth (expected) information. However, the MPC system performed 30 times slower due to the optimum search convergence and bias in the $Fref$ reference profile. Such MPC slowness was not noticeable in ideal scenarios with no randomization. However, the latter, as well as the extremum pursuit routines, were not necessary when utilizing an approach that uses first principles. Finally, qualitatively speaking, both the adaptive PI that used first principles and the MPC produced repeatable outcomes; thus, robustness was confirmed.

6. Conclusions

This paper develops an adaptive control system for the setpoint control of the biomass specific growth rate, i.e., SGR, in fed-batch cultivation processes (in which a linear PI controller is applied for nonlinear process control). The feedback signal for the system controller was obtained from the OUR measurements-based SGR estimator, as well as from the digital twin numerical simulation. The controller adaptation was based on a first principles model of a controlled process, specifically one that is linearized around the current state. The resultant dynamic parameters of the linearized model were updated online with the measured values of the process variables, and these were then directly applied for the tuning rules-based adaptation of controller parameters.

The SGR control system was tested using numeric simulation. Overall, the SGR control precision was tested by comparing the resulting biomass concentration with the experimental data. The following results were obtained: 1.154 g kg^{-1} for the MAE indicator and 3.145% for the RMSE. The SGR signal tracking errors were negligible. For comparison, the MPC controller was also implemented and tested on the same digital twin infrastructure. Both methods demonstrated similar qualitative outcomes and confirmed their robustness. However, the randomization of the controller parameters caused a convergence slowness in the MPC execution. Meanwhile, the adaptive PI that used first principles had no performance issues, and it was approximately 30 times faster in contrast to the MPC. Therefore, the developed SGR control system can be applied to control various fed-batch cultures, i.e., where the slowness caused by optimum search implementations is not acceptable.

Table 5
Results of the digital twin and control during validation when the feedback was modeled by Equations (34) and (37).

Exp. no.	Biomass conc.		Glucose conc.		OUR		Feeding rate	
	MAE g kg^{-1}	NRMSE %	MAE g kg^{-1}	NRMSE %	MAE g kg^{-1}	NRMSE %	MAE g kg^{-1}	NRMSE %
E. coli BL21 (DE3) pET21-IFN-alfa-5								
1	0.895	2.618	0.057	2.317	0.373	5.733	5.392	3.357
2	0.792	1.755	0.068	2.844	0.276	1.648	6.934	4.199
3	0.577	1.348	0.111	4.117	0.582	5.791	5.749	2.728
4	0.467	0.958	0.052	2.221	0.358	3.949	4.609	2.188
5	0.713	1.729	0.052	2.366	0.387	4.617	4.976	2.729
6	0.723	1.669	0.142	3.568	0.312	3.703	4.698	3.169
7	0.538	2.157	0.157	4.551	0.281	5.394	5.155	3.289
8	1.116	3.613	0.286	8.533	0.522	5.449	6.124	3.572
E. coli BL21 (DE3) pET28a								
1	0.974	3.921	0.089	2.518	0.416	7.165	2.489	5.185
2	1.321	5.039	0.219	3.819	0.367	6.064	2.941	5.463
3	1.738	6.269	0.339	7.305	0.363	6.204	2.127	5.466
4	1.059	3.999	0.274	5.268	0.527	7.710	4.733	6.507
5	0.813	3.285	0.224	5.215	0.418	6.250	2.810	5.725
6	0.797	3.433	0.181	3.799	0.316	5.557	3.465	6.149
7	2.044	6.313	0.371	12.84	0.632	6.039	2.646	4.751

Table 6
Results of digital twin and control during the validation when the SGR feedback is estimated.

Exp. no.	Biomass conc.		Glucose conc.		OUR		Feeding rate	
	MAE g kg^{-1}	NRMSE %	MAE g kg^{-1}	NRMSE %	MAE g kg^{-1}	NRMSE %	MAE g kg^{-1}	NRMSE %
E. coli BL21 (DE3) pET21-IFN-alfa-5								
1	0.598	1.378	0.057	2.313	0.364	5.298	5.606	2.889
2	1.617	3.311	0.068	2.836	0.405	1.848	5.861	3.159
3	0.831	1.976	0.111	4.108	0.393	4.381	7.068	2.872
4	1.380	3.414	0.053	2.221	0.493	5.024	8.696	3.720
5	1.599	3.653	0.052	2.366	0.566	5.957	7.326	3.525
6	1.158	2.805	0.142	3.568	0.325	3.241	5.506	2.932
7	1.041	1.359	0.156	4.550	0.382	2.042	5.475	2.735
8	0.573	1.515	0.285	8.511	0.203	2.225	4.817	2.305
E. coli BL21 (DE3) pET28a								
1	1.444	3.921	0.091	2.517	0.536	7.165	3.434	5.185
2	1.756	5.039	0.215	3.819	0.371	6.064	3.838	5.463
3	2.203	6.269	0.339	7.305	0.361	6.204	3.362	5.465
4	1.254	3.999	0.267	5.268	0.617	7.710	4.959	6.507
5	1.075	3.284	0.244	5.215	0.474	6.250	4.153	5.725
6	1.045	3.433	0.181	3.799	0.399	5.557	4.243	6.149
7	2.464	6.313	0.371	12.84	0.739	6.039	3.475	4.751

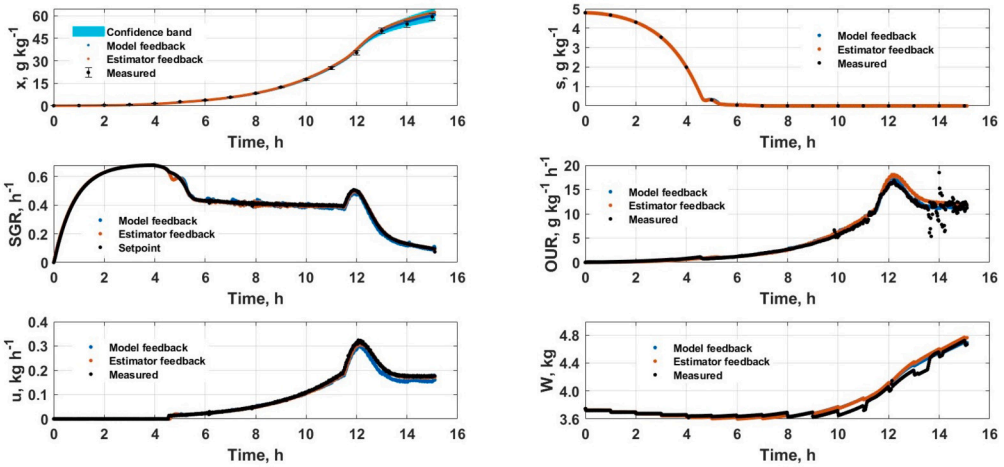

Fig. 6. The graphical view of the cultivation process #3 data of the *E. coli* BL21 (DE3) pET21-IFN-alfa-5 strain and of the SGR control system results with the two different types of SGR feedback.

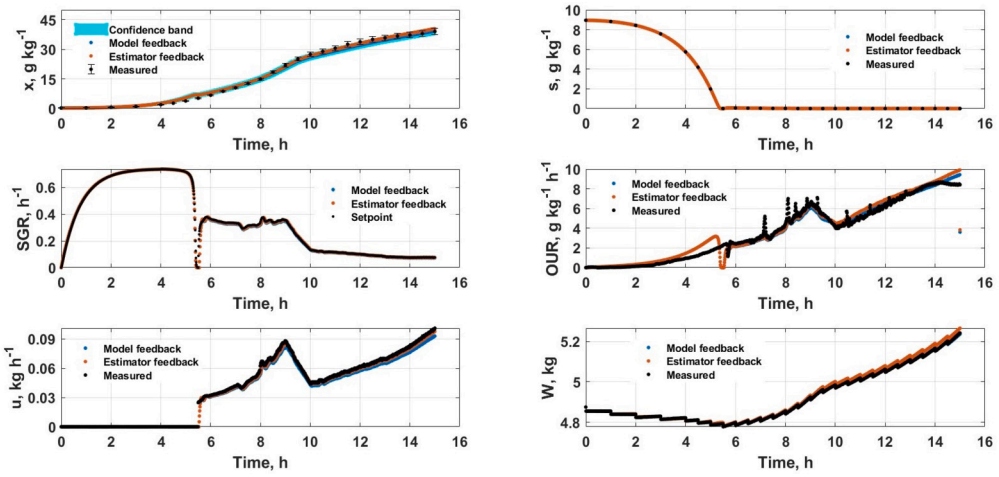

Fig. 7. The graphical view of the cultivation process #5 data of the *E. coli* BL21 (DE3) pET28a strain and the SGR control system results with the two different types of feedback.

Table 7
Comparison of the results of this study when using the MPC [49].

The source	Biomass conc. NRMSE %	OUR NRMSE %
This study (first principles)	3.145	5.238
MPC [49]	9.1	14.4

In the scenarios when computation duration is not an issue and the target strain culture is well known, the MPC approach is more rational to use when less bias is a more considerable preference in the operated systems.

CRediT authorship contribution statement

Conceptualization, D.L. and R.U.; methodology, D.L. and R.U.; software, A.S. and D.M.; validation, D.M. and D.G.; formal analysis, D.M. and P.B.; investigation, D.L. and D.M.; resources, R.U.; data curation, P.B., D.G., and A.S.; writing—original draft preparation, D.L., D.M., and R.U.; writing—review and editing, R.U. and A.S.; visualization, A.S., D.G., and P.B.; supervision, R.U. All authors have read and agreed to the published version of the manuscript.

Declaration of competing interest

We declare no conflicts of interest when submitting our paper "Adaptive control of *E. coli* specific growth rate in fed-batch cultivation based on oxygen uptake rate" for publishing it in the Computational and Structural Biotechnology journal.

Funding

This project received funding from the European Regional Development Fund (project no. 01.2.2-LMT-K-718-03-0039) under a grant agreement with the Research Council of Lithuania (LMTLT).

References

[1] Sonnleitner B, Kappeli O. Growth of saccharomyces cerevisiae is controlled by its limited respiratory capacity: formulation and verification of a hypothesis. Biotechnol Bioeng 1986;28(6):927–37. https://doi.org/10.1002/bit.260280620.
[2] Rocha I, Veloso A, Carneiro S, Costa R, Ferreira E. Implementation of a specific rate controller in a fed-batch e. coli fermentation. IFAC Proceedings Volumes 2008;41(2):15565–70. https://doi.org/10.3182/20080706-5-KR-1001.02632.
[3] Gnoth S, Jenzsch M, Simutis R, Lübbert A. Control of cultivation processes for recombinant protein production: a review. Bioprocess Biosyst Eng 2008;31(1):21–39. https://doi.org/10.1007/s00449-007-0163-7.
[4] Gregory ME, Turner C. Open-loop control of specific growth rate in fed-batch cultures of recombinant e.coli. Biotechnol Tech 1993;7(12):889–94. https://doi.org/10.1007/BF00156368.
[5] Chenikher S, Guez J, Coutte F, Pekpe M, Jacques P, Cassar J. Control of the specific growth rate of bacillus subtilis for the production of biosurfactant lipopeptides in bioreactors with foam overflow. Process Biochem 2010;45(11):1800–7. https://doi.org/10.1016/j.procbio.2010.06.001.
[6] Picó-Marco E, Picó J, De Battista H. Sliding mode scheme for adaptive specific growth rate control in biotechnological fed-batch processes. Int J Control 2005;78(2):128–41. https://doi.org/10.1080/00207170500073772.
[7] De Battista H, Picó J, Picó-Marco E. Nonlinear PI control of fed-batch processes for growth rate regulation. J Process Control 2012;22(4):789–97. https://doi.org/10.1016/j.jprocont.2012.02.011.
[8] Jenzsch M, Simutis R, Luebbert A. Generic model control of the specific growth rate in recombinant escherichia coli cultivations. J Biotechnol 2006;122(4):483–93. https://doi.org/10.1016/j.jbiotec.2005.09.013.
[9] Dabros M, Schuler MM, Marison IW. Simple control of specific growth rate in biotechnological fed-batch processes based on enhanced online measurements of biomass. Bioprocess Biosyst Eng 2010;33(9):1109–18. https://doi.org/10.1007/s00449-010-0438-2.
[10] Brignoli Y, Freeland B, Cunningham D, Dabros M. Control of specific growth rate in fed-batch bioprocesses: novel controller design for improved noise management. Processes 2020;8(6):679. https://doi.org/10.3390/pr8060679.
[11] Deployment of metabolic heat rate based soft sensor for estimation and control of specific growth rate in glycoengineered pichia pastoris for human interferon alpha 2b production. J Biotechnol 2022;359:194–206. https://doi.org/10.1016/j.jbiotec.2022.10.006.
[12] Kuprijanov A, Schaepe S, Aehle M, Simutis R, Lübbert A. Improving cultivation processes for recombinant protein production. Bioprocess Biosyst Eng 2012;35(3):333–40. https://doi.org/10.1007/s00449-011-0571-6.
[13] Soons Z, Voogt J, van Straten G, van Boxtel A. Constant specific growth rate in fed-batch cultivation of bordetella pertussis using adaptive control. J Biotechnol 2006;125(2):252–68. https://doi.org/10.1016/j.jbiotec.2006.03.005.
[14] Craven S, Whelan J, Glennon B. Glucose concentration control of a fed-batch mammalian cell bioprocess using a nonlinear model predictive controller. J Process Control 2014;24(4):344–57. https://doi.org/10.1016/j.jprocont.2014.02.007.
[15] Aehle M, Bork K, Schaepe S, Kuprijanov A, Horstkorte R, Simutis R, et al. Increasing batch-to-batch reproducibility of CHO-cell cultures using a model predictive control approach. Cytotechnology 2012;64(6):623–34. https://doi.org/10.1007/s10616-012-9438-1.
[16] Levisauskas D, Simutis R, Borvitz D, Lübbert A. Automatic control of the specific growth rate in fed-batch cultivation processes based on an exhaust gas analysis. Bioprocess Eng 1996;15(3):145–50. https://doi.org/10.1007/BF00369618.
[17] Levisauskas D. Inferential control of the specific growth rate in fed-batch cultivation processes. Biotechnol Lett 2001;23:1189–95. https://doi.org/10.1023/a:1010528915228.
[18] Galvanauskas, Simutis, Levišauskas, Urniežius. Practical solutions for specific growth rate control systems in industrial bioreactors. Processes 2019;7(10):693. https://doi.org/10.3390/pr7100693.
[19] Abadli M, Dewasme L, Tebbani S, Dumur D, Wouwer AV. Generic model control applied to e. coli bl21(de3) fed-batch cultures. Processes 2020;8(7):772. https://doi.org/10.3390/pr8070772.
[20] Dewasme L, Fernandes S, Amribt Z, Santos L, Bogaerts P, Wouwer AV. State estimation and predictive control of fed-batch cultures of hybridoma cells. J Process Control 2015;30:50–7. https://doi.org/10.1016/j.jprocont.2014.12.006.

[21] Valentinotti S, Srinivasan B, Holmberg U, Bonvin D, Cannizzaro C, Rhiel M, et al. Optimal operation of fed-batch fermentations via adaptive control of overflow metabolite. Control Eng Pract 2003;11(6):665–74. https://doi.org/10.1016/s0967-0661(02)00172-7.
[22] Renard F, Wouwer AV, Perrier M. Robust adaptive control of yeast fed-batch cultures. IFAC Proc Vol 2006;39(2):189–94. https://doi.org/10.3182/20060402-4-br-2902.00189.
[23] Dewasme L, Richelle A, Dehottay P, Georges P, Remy M, Bogaerts P, et al. Linear robust control of s. cerevisiae fed-batch cultures at different scales. Biochem Eng J 2010;53(1):26–37. https://doi.org/10.1016/j.bej.2009.10.001.
[24] Hocalar A, Turker M. Model based control of minimal overflow metabolite in technical scale fed-batch yeast fermentation. Biochem Eng J 2010;51(1–2):64–71. https://doi.org/10.1016/j.bej.2010.04.014.
[25] Martinez C, Gouze J-L. Optimal control of a fed-batch reactor with overflow metabolism. IFAC-PapersOnLine 2020;53(2):16820–5. https://doi.org/10.1016/j.ifacol.2020.12.1167.
[26] Abadli M, Dewasme L, Tebbani S, Dumur D, Wouwer AV. An experimental assessment of robust control and estimation of acetate concentration in escherichia coli BL21(DE3) fed-batch cultures. Biochem Eng J 2021;174:108103. https://doi.org/10.1016/j.bej.2021.108103.
[27] Urniezius R, Galvanauskas V, Survyla A, Simutis R, Levisauskas D. From physics to bioengineering: microbial cultivation process design and feeding rate control based on relative entropy using nuisance time. Entropy 2018;20(10):779. https://doi.org/10.3390/e20100779.
[28] Survyla A, Urniezius R, Simutis R. Viable cell estimation of mammalian cells using off-gas-based oxygen uptake rate and aging-specific functional. Talanta 2023;254:124121. https://doi.org/10.1016/j.talanta.2022.124121.
[29] Biechele P, Busse C, Solle D, Scheper T, Reardon K. Sensor systems for bioprocess monitoring. Eng Life Sci 2015;15(5):469–88. https://doi.org/10.1002/elsc.201500014.
[30] Claßen J, Aupert F, Reardon KF, Solle D, Scheper T. Spectroscopic sensors for in-line bioprocess monitoring in research and pharmaceutical industrial application. Anal Bioanal Chem 2016;409(3):651–66. https://doi.org/10.1007/s00216-016-0068-x.
[31] Ude C, Schmidt-Hager J, Findeis M, John G, Scheper T, Beutel S. Application of an online-biomass sensor in an optical multisensory platform prototype for growth monitoring of biotechnical relevant microorganism and cell lines in single-use shake flasks. Sensors 2014;14(9):17390–405. https://doi.org/10.3390/s140917390.
[32] Habegger L, Crespo KR, Dabros M. Preventing overflow metabolism in crabtree-positive microorganisms through on-line monitoring and control of fed-batch fermentations. Fermentation 2018;4(3):79. https://doi.org/10.3390/fermentation4030079.
[33] Galvanauskas V, Simutis R, Vaitkus V. Adaptive control of biomass specific growth rate in fed-batch biotechnological processes. a comparative study. Processes 2019;7(11):810. https://doi.org/10.3390/pr7110810.
[34] Urniezius R, Survyla A, Paulauskas D, Bumelis VA, Galvanauskas V. Generic estimator of biomass concentration for escherichia coli and saccharomyces cerevisiae fed-batch cultures based on cumulative oxygen consumption rate. Microb Cell Fact 2019;18(1):190. https://doi.org/10.1186/s12934-019-1241-7.
[35] Kumar J, Bhat SU, Rathore AS. Slow post-induction specific growth rate enhances recombinant protein expression in escherichia coli: pramlintide multimer and ranibizumab production as case studies. Process Biochem 2022;114:21–7. https://doi.org/10.1016/j.procbio.2022.01.009.
[36] Kim JW, Krausch N, Aizpuru J, Barz T, Lucia S, Neubauer P, et al. Model predictive control and moving horizon estimation for adaptive optimal bolus feeding in high-throughput cultivation of e. coli. Comput Chem Eng 2023;172:108158. https://doi.org/10.1016/j.compchemeng.2023.108158.
[37] Survyla A, Levisauskas D, Urniezius R, Simutis R. An oxygen-uptake-rate-based estimator of the specific growth rate in escherichia coli BL21 strains cultivation processes. Comput Struct Biotechnol J 2021;19:5856–63. https://doi.org/10.1016/j.csbj.2021.10.015.
[38] Urniezius R, Survyla A. Identification of functional bioprocess model for recombinant e. coli cultivation process. Entropy 2019;21(12):1221. https://doi.org/10.3390/e21121221.
[39] Garcia-Ochoa F, Gomez E, Santos VE, Merchuk JC. Oxygen uptake rate in microbial processes: an overview. Biochem Eng J 2010;49(3):289–307. https://doi.org/10.1016/j.bej.2010.01.011.
[40] Luedeking R, Piret EL. Transient and steady states in continuous fermentation. Theory and experiment. J Biochem Microbiol Technol Eng 1959;1(4):431–59. https://doi.org/10.1002/jbmte.390010408.
[41] Urniezius R, Kemesis B, Simutis R. Bridging offline functional model carrying aging-specific growth rate information and recombinant protein expression: entropic extension of Akaike information criterion. Entropy 2021;23(8):1057. https://doi.org/10.3390/e23081057.
[42] Smaluch K, Wollenhaupt B, Steinhoff H, Kohlheyer D, Grünberger A, Dusny C. Assessing the growth kinetics and stoichiometry of Escherichia coli at the single-cell level. Eng Life Sci 2023;23(1). https://doi.org/10.1002/elsc.202100157.
[43] Monod J. The growth of bacterial cultures. Annu Rev Microbiol 1949;3(1):371–94. https://doi.org/10.1146/annurev.mi.03.100149.002103.
[44] Astrom KJ, Hagglund. PID controllers. 2nd edition. International Society for Measurement and Control; 1995.
[45] Galvanauskas V, Simutis R, Levisauskas D, Butkus M, Urniezius R. Development and investigation of efficient substrate feeding and dissolved oxygen control algorithms for design of recombinant e. coli cultivation process. In: 2018 IEEE 14th international conference on automation science and engineering (CASE). IEEE. p. 657–60. https://doi.org/10.1109/COASE.2018.8560495.
[46] Guthrie WF. NIST/SEMATECH e-handbook of statistical methods. NIST handbook, vol. 151. 2020. https://doi.org/10.18434/M32189.
[47] Warwick K. Industrial digital control systems. Comprehensively rev. edition, vol. 37. Peregrinus; 1988.
[48] Abadli M, Dewasme L, Tebbani S, Dumur D, Wouwer AV. Experimental validation of a nonlinear model predictive controller regulating the acetate concentration in fed-batch escherichia coli BL21(DE3) cultures. Adv Control Appl 2022;4(1). https://doi.org/10.1002/adc2.95.
[49] Ulonska S, Waldschitz D, Kager J, Herwig C. Model predictive control in comparison to elemental balance control in an e. coli fed-batch. Chem Eng Sci 2018;191:459–67. https://doi.org/10.1016/j.ces.2018.06.074.
[50] Willmott C, Matsuura K. Advantages of the mean absolute error (MAE) over the root mean square error (RMSE) in assessing average model performance. Clim Res 2005;30:79–82. https://doi.org/10.3354/cr030079.